

# Two-dimensional bosonic droplets in a harmonic trap

Fabian Brauneis,<sup>1</sup> Artem G. Volosniev,<sup>2</sup> and Hans-Werner Hammer<sup>1,3</sup>

<sup>1</sup>*Technische Universität Darmstadt, Department of Physics, 64289 Darmstadt, Germany*

<sup>2</sup>*Department of Physics and Astronomy, Aarhus University,  
Ny Munkegade 120, DK-8000 Aarhus C, Denmark*

<sup>3</sup>*ExtreMe Matter Institute EMMI and Helmholtz Forschungsakademie Hessen für FAIR (HFHF),  
GSI Helmholtzzentrum für Schwerionenforschung GmbH, 64291 Darmstadt, Germany*

We investigate a system of bosons in a two-dimensional harmonic trap. In the limit of strong attractive interactions, the bosons make a droplet insensitive to external confinement. For weak interactions, in contrast, the ground state is given by the harmonic trap. In this work, we conduct a variational study of the transition between these two limits. We find that this transition occurs abruptly at the critical interaction strength whose value is universal if scaled appropriately with the number of particles. To connect the abrupt change in the properties of the system to the classical description of phase transitions, we analyze the static response of the Bose gas related to the isothermal compressibility. Finally, we perform numerically exact calculations for a few particles to demonstrate the effects of finite range interactions on this transition. We conclude that finite range effects wash out the point of transition.

## I. INTRODUCTION

Twenty years ago, Hammer and Son predicted a universal many-body bound state for a large, but finite number of attractively interacting bosons in two spatial dimensions (2D) [1]. They found that upon addition of another boson to the system, the bound-state energy decreases by a factor of  $E_{N+1}/E_N = 8.567$  while the characteristic size shrinks by  $R_{N+1}/R_N = 0.3417$ . The analysis was based on a mean-field approach that used the scale invariance of the contact interaction in 2D by introducing a renormalization group (RG) improved running coupling constant. These results were later confirmed by *ab initio* calculations [2–4]. A possible platform for the experimental realization of such a system are cold atoms. Indeed, two-dimensional systems with bosons have been created experimentally, see e.g. Ref. [5]; few-body cold-atom systems have also been studied, albeit mainly fermions [6–9].

The crucial difference between the standard cold-atom experiments and the system of Ref. [1] is the presence of a harmonic confinement, which introduces another length scale into the problem. This means that the results of Ref. [1] are only applicable for interactions strong enough (corresponding to sufficiently small values of  $R_N$ ) that the effect of the trapping potential can be neglected. For weak interactions, the properties of the system are dictated by the trapping potential. The goal of our study is to provide insight into the transition between these two cases. In particular, we show that this transition contains information about universality of the many-body bound states in 2D, providing a route for experimental studies of the corresponding physics.

To facilitate such studies, this paper provides an intuitive physical picture based upon a simple variational ansatz that incorporates the information about the trapping potential and the RG-improved coupling constant. As consequence, both the harmonic oscillator ground state and the universal many-body bound state are accurately described in the limiting cases. The transition

between the two states is induced by changing either of the two tunable experimental parameters: The scattering length (e.g. through Feshbach resonances [10]) and the trapping frequency, see Fig. 1. To characterize the transition, we introduce an observable which is closely related to the compressibility of the Bose gas [11]. This observable, the static response, distinguishes the two states of the system and can be measured by changing the trapping frequency [12, 13]. Finally, we will discuss the impact of finite range effects on this transition by performing *ab initio* calculations in the few-body sector.

We note a relevant recent study [14] where bosonic droplets were studied on the surface of a sphere whose curvature naturally acts as an additional length scale. It was shown, in particular using Monte Carlo simulations, that for a finite but large particle number, an analogue of a first order phase transition occurs between a homogeneously distributed ground state and a localized droplet. The results of Ref. [14] will be used to motivate certain aspects of the variational ansatz employed in the present paper.

The paper is structured as follows: In Sec. II we introduce the system and clarify the physics of the problem. Further, we explain the methods employed in the present study. Our main results are presented in Sec. III. Section IV briefly summarizes our findings and gives an outlook into future research perspectives. Further technical details are provided in two Appendices.

## II. FORMULATION AND METHODS

### A. System

We consider a system of attractively interacting bosons in a two-dimensional harmonic trap

$$H = \int d\vec{x} \left[ \frac{\hbar^2}{2m} |\nabla\psi(\vec{x})|^2 + \frac{m\omega^2 \vec{x}^2}{2} |\psi(\vec{x})|^2 + W \right], \quad (1)$$

where  $\psi(\vec{x})$  is the bosonic field annihilation operator with  $N = \int d^2x \psi^\dagger(\vec{x})\psi(\vec{x})$ , the number of bosons. The operator  $W$  is the boson-boson interaction  $W = -\int d\vec{x}' \psi^\dagger(\vec{x})\psi^\dagger(\vec{x}')V(\vec{x} - \vec{x}')\psi(\vec{x}')\psi(\vec{x})$ , where the positive function  $V$  describes the interaction potential. In the main part of this work, we assume zero-range interactions,  $V(\vec{x} - \vec{x}') = g\delta(\vec{x} - \vec{x}')$  with  $g > 0$ . Such interactions are typically used in the description of ultra cold gases [15, 16]. In Sec. III C, we will also illustrate influence of finite range effects.

We use a system of units such that  $\hbar = m = 1$ . However, we keep the trapping frequency, i.e., we will give lengths in the units of the harmonic oscillator length  $l_{\text{HO}} = \sqrt{\frac{1}{\omega}}$  and energies in the units of  $\omega$ . For a sketch of the system see Fig. 1.

The effective range expansion in two dimensions has a logarithmic dependence on the scattering length [17], or more precisely, on  $\ln(ka)$  with  $a$  the scattering length and  $k$  the wave number. This implies that the interaction strength  $g$  in two dimensions is a function of the considered length/momentum scales. In Ref. [1] standard renormalization group arguments are used to introduce a coupling constant for a many-body problem which ‘runs’ with the many-body ground state energy  $E$  via

$$g(R) = -\frac{4\pi}{\ln(R^2 B_2)}, \quad (2)$$

where  $R$  is the characteristic length of the ground state, which is connected to  $E$  by  $E \sim 1/R^2$ . Furthermore,  $g(R)$  depends on the two-body binding energy in free space  $B_2 = -E_2^1$ . This equation implies that for a given two-body binding energy  $B_2$ , the size of the many-body bound state (its energy) determines the interaction strength such that the size is maximal (energy minimal). Therefore, in what follows we will use  $B_2$  as the relevant scale for the interaction.

### Basic Physical Considerations

We start by providing some physical intuition into the properties of the system. However, first let us summarize the results of Ref. [1] where Eq. (1) was studied without an external trapping potential, i.e., with  $\omega = 0$ . In this work, first, the energy dependent coupling constant, Eq. (2), was introduced, which effectively replaced the bare interaction by the full multiple scattering series. Then, the many-body problem was solved using a mean-field ansatz,  $\psi(\vec{x}) \sim \Psi(\vec{x})$ , with  $\Psi(\vec{x})$  a single particle orbital occupied by all particles:

$$\Psi(\vec{x}) = \frac{\sqrt{N}}{R_{\text{free}}\sqrt{2\pi C}} f_{\text{free}}(r/R_{\text{free}}), \quad (3)$$

<sup>1</sup> Note that the two-body binding energy can be used to define the 2D scattering length  $a = 2e^{-\gamma}\sqrt{1/B_2}$  [17], where  $\gamma$  is the Euler-Mascheroni constant.

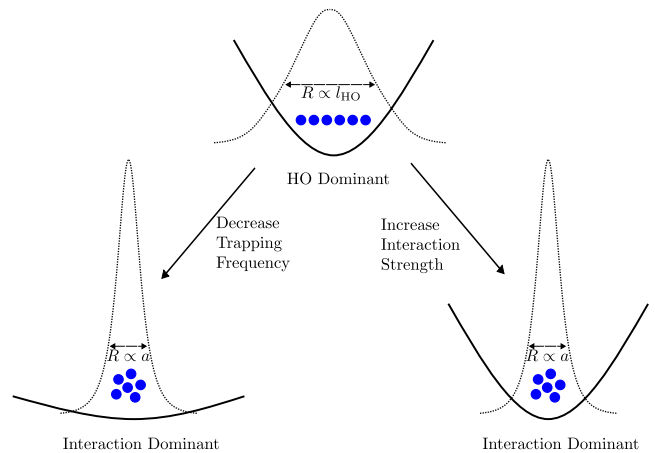


FIG. 1. Sketch of the system. Blue spheres represent  $N$  attractively interacting bosons. The solid curve is the trapping potential. The dashed curve illustrates the density of the bosons. For the trap-dominant regime, the density profile is given by a Gaussian. For the interaction-dominant regime, the solution follows Ref. [1]; it has an exponential decaying tail. The characteristic size is given in the former case by the harmonic oscillator length  $l_{\text{HO}}$  while in the latter case it is proportional to the scattering length  $a$ . As sketched, a change from the trap-dominant to the interaction-dominant regime can be induced by either increasing the interaction strength or by decreasing the trapping frequency.

with  $r \equiv |\vec{x}|$ . The constant  $C$  is determined by the particle number constraint,  $C = \int d\rho \rho f_{\text{free}}^2(\rho)$ .

The unknowns  $R_{\text{free}}$  and  $f_{\text{free}}$  in Eq. (3) are found by minimizing the expectation value of the Hamiltonian  $H$

$$E(R_{\text{free}}) = \frac{A}{2C} \frac{N}{R_{\text{free}}^2} - \frac{B}{4\pi C^2} \frac{g(R_{\text{free}})N^2}{R_{\text{free}}^2}, \quad (4)$$

where  $A = \int d\rho \rho [f'_{\text{free}}(\rho)]^2$ ,  $B = \int d\rho \rho f_{\text{free}}^4(\rho)$ . The parameter  $R_{\text{free}}$  depends on  $N$ , and we shall use a subscript  $N$  to indicate this fact explicitly when needed. For large values of  $N$ , this minimization demonstrated the existence of a universal bound state with the shape  $f_{\text{free}}$  independent on the number of particles. The corresponding energies and length scales obey  $E_{N+1}/E_N = 8.567$  and  $R_{\text{free},N+1}/R_{\text{free},N} = 0.3417$ .

If we follow the steps of Ref. [1] for a system with the harmonic trapping potential, we obtain instead of Eq. (4)

$$E(R) = \frac{A}{2C} \frac{N}{R^2} - \frac{B}{4\pi C^2} \frac{g(R)N^2}{R^2} + \frac{R^2}{l_{\text{HO}}^4} \frac{ND}{2C} \quad (5)$$

with  $D = \int d\rho \rho^3 f^2(\rho)$ . This equation contains the physics of the system for limiting values of the new length scale  $l_{\text{HO}}$ . For strong interactions, we have  $R_{\text{free}} \ll l_{\text{HO}}$  and the effect of the harmonic trap is negligible. In this case, the system is described by Eq. (4). For weak interactions, the size of the many-body bound state in free space becomes considerably larger than the harmonic oscillator length. Therefore, the state has to be restricted

by the new length scale so that  $R \approx l_{\text{HO}}$  and  $f \approx f_{\text{HO}}$ , the ground state of the 2D harmonic oscillator. In this case, the interaction term becomes negligible, and the ground state of the system is determined by the external trapping potential. We sketch these limiting cases in Fig. 1.

## B. Methods

### Variational Ansatz

Motivated by the discussion above, we propose the variational ansatz<sup>2</sup>

$$\Psi(\vec{x}) = \frac{1}{\mathcal{N}} [\alpha_{\text{HO}} f_{\text{HO}}(r) + \alpha_{\text{free}} f_{\text{free}}(r/R)] \quad (6)$$

to study the transition between the two states of the system. The function  $f_{\text{HO}}$  describes the ground state of a harmonic oscillator,

$$f_{\text{HO}}(r) = \frac{1}{l_{\text{HO}}\sqrt{\pi}} e^{-\frac{r^2}{2l_{\text{HO}}^2}}, \quad (7)$$

and  $f_{\text{free}}$  is the shape found in Ref. [1] for the universal many-body bound state;  $\alpha_{\text{HO}}$  and  $\alpha_{\text{free}}$  are variational parameters,  $\mathcal{N}$  is a normalization coefficient, see App. A. The characteristic width of the state, is given by  $R$ . Following our physical insight we use  $R = R_{\text{free}}$  if  $R_{\text{free}}$  is smaller than the harmonic oscillator length. If it is larger, the characteristic length scale of the ground state is determined by the harmonic oscillator, so we use  $R = l_{\text{HO}}$  instead. We calculate  $R_{\text{free}}$  by minimizing the energy functional of Eq. (4) using the shape  $f_{\text{free}}$  for the calculation of  $A, B, C$ .

To find the values of  $\alpha_{\text{HO}}$  and  $\alpha_{\text{free}}$  we minimize the expectation value of  $H$  for a given interaction strength, i.e., for a given two-body binding energy in free space  $B_2/\omega$ . This procedure will allow us to analyze the transition between the harmonic oscillator and the many-body bound state (see below). For a more detailed explanation of the employed variational ansatz including all relevant equations see App. A.

### Configuration interaction method

In Sec. III C we study the influence of finite range effects on the transition. To that end, we perform an *ab*

*initio* calculation by employing the configuration interaction (CI) method [18, 19]. Instead of the contact interaction, we use a Gaussian interaction potential, which reads as

$$V(\vec{x}) = \frac{g}{2\pi\sigma^2} e^{-\vec{x}^2/2\sigma^2}, \quad (8)$$

$g > 0$ ,  $\sigma > 0$ , in Eq. (1). To be able to compare with the results obtained with a contact interaction, we calculate  $B_2$  by expanding the two-body Schrödinger equation in free space using the harmonic oscillator eigenfunctions and subsequently diagonalizing the Hamiltonian matrix. We provide an explanation of our CI calculations in App. B.

To estimate finite range effects of the Gaussian potential, we use the expression [20]:

$$B_2 = -\frac{1}{r_{\text{eff}}^2} W\left(-2e^{-2\gamma} \frac{r_{\text{eff}}^2}{a^2}\right), \quad (9)$$

where  $r_{\text{eff}}$  is the effective range and  $W$  is the product logarithm (also known as the Lambert  $W$  function, defined as the solution of  $z = we^w$  with  $W(z) = w$ ). We estimate the scattering length using the semi-analytical expressions of Ref. [21]. Then, we calculate the effective range by solving Eq. (9) using the scattering length and the numerically calculated two-body ground state energy in free space.

## III. RESULTS

### A. Minimization of variational ansatz

Here, we discuss the outcome of the minimization procedure for the variational ansatz discussed above.

#### Comparison with perturbation theory

In Fig. 2 we show typical results from the minimization of our ansatz, Eq. (6), together with perturbation theory for  $N = 9$  bosons as a function of the two-body energy in free space  $B_2/\omega$ . Perturbation theory can be constructed for the two limiting cases discussed above, i.e.,  $B_2/\omega \rightarrow 0$  (weak boson-boson interactions) and  $B_2/\omega \rightarrow \infty$  (strong boson-boson interaction).

For weak interactions, all bosons occupy the ground state of a harmonic oscillator and we treat the contact interaction as perturbation

$$E(B_2/\omega \rightarrow 0) = N\omega - \frac{g(R=l_{\text{HO}})}{2} N^2 \int d^2x f_{\text{HO}}(\vec{x})^4. \quad (10)$$

Note that this integral can be evaluated analytically:  $E(B_2/\omega \rightarrow 0) = N\omega - \frac{g(R=l_{\text{HO}})}{4\pi} N^2$ . We have used that the characteristic width of the state of our system,  $R$ , is given by the harmonic oscillator length, i.e.  $R = l_{\text{HO}}$ . In the opposite limit of strong boson-boson attraction,

<sup>2</sup> Note that we also studied the system with another ansatz (not reported here) where both shapes scale with  $R$ ,  $\Psi(\vec{r}) \sim \alpha_{\text{HO}} f_{\text{HO}}(r/R) + \alpha_{\text{free}} f_{\text{free}}(r/R)$ . We observed that this ansatz supports the main conclusions presented in the paper. However, there is an important difference between the two approaches: The ansatz in Eq. (6) leads to a sharp transition from the trap-dominant to the interaction-dominant regimes in agreement with Ref. [14].

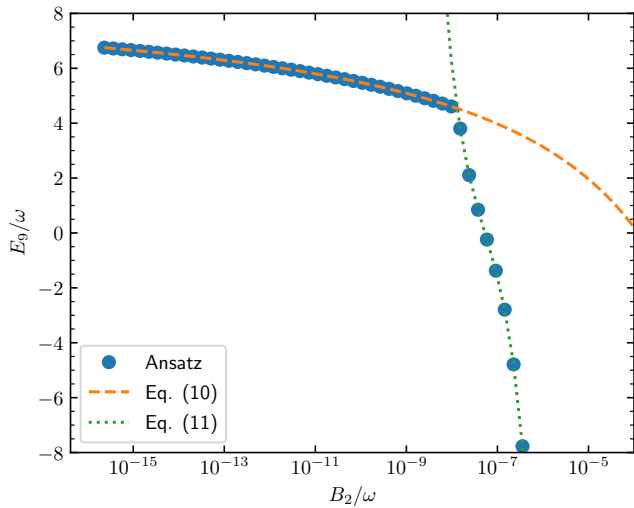


FIG. 2. Energy for  $N = 9$  bosons calculated with our ansatz, Eq. (6), together with the outcome of perturbation theory, see Eqs. (10) and (11).

we instead treat the harmonic oscillator potential as a perturbation to the universal many-body bound state

$$E(B_2/\omega \rightarrow \infty) = E(R_{\text{free}}) + \frac{\omega^2 ND}{2C} R_{\text{free}}^2 \quad (11)$$

with  $E(R_{\text{free}})$  from Eq. (4). Figure 2 demonstrates that perturbation theory is in excellent agreement with our ansatz, and can be used to study energies in a simple manner.

In particular, we can use perturbation theory to estimate the transition point, i.e., the crossing in Fig. 2. Searching for the interaction strength at which the energies in Eqs. (10) and (11) are identical reveals that the transition happens at  $R_{\text{free}} = l_{\text{HO}}$ . This is also the outcome of the minimization calculation. Using Eq. (2) and  $g(R_{\text{free}}) = \frac{2\pi AC}{NB}$ , the expression found in Ref. [1] for large values of  $N$ , it follows that the transition should happen at

$$\frac{\ln(B_2/\omega)}{N} = -2.148. \quad (12)$$

The fact that  $\ln(B_2/\omega)/N$  is constant at the transition point suggests that this quantity is the proper measure of the interaction strength for our study. As we show below, for increasing values of  $N$  the transition point converges indeed to this value. This is also in agreement with Ref. [14], which showed that with increasing particle number, the transition between the non-interacting state and the universal many-body bound state converges to  $\ln(B_2/\tilde{E})/N = -2.148 + \mathcal{O}(1/N)$ , where  $\tilde{E}$  is the relevant energy scale in that work. This showcases the universality of the transition point even for different systems.

An inspection of the variationally optimized values of  $\alpha_{\text{HO}}$  and  $\alpha_{\text{free}}$  shows that for all particle numbers and

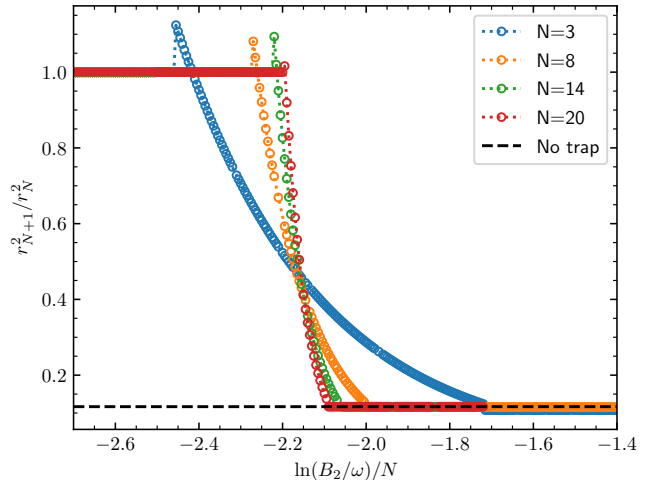


FIG. 3. Ratio of the mean-square radius  $r_{N+1}^2/r_N^2$  as a function of the interaction strength given by  $\ln(B_2/\omega)/N$ . The symbols are the results obtained from the minimization of the energy with our ansatz, see Eq. (6). The black dashed line is the universal prediction from Ref. [1]. Dotted lines are added to guide the eye.

all interactions one of these parameters is always zero, i.e., for every interaction strength the ground state of the system is described by either  $f_{\text{HO}}$  or  $f_{\text{free}}$  (see also App. B). This means that we have a sharp transition between the two states for all particle numbers. This is a deliberately chosen feature of our ansatz motivated by the results of Ref. [14] for bosons on a sphere. Note that in reality a sharp transition can occur only for large particle numbers,  $N \gg 1$ ; for small particle numbers the ground state energy should be a smooth function of the parameters<sup>3</sup>.

#### Ratio of the radii

In Fig. 3 we show the ratio of the mean-square radius  $r_{N+1}^2/r_N^2$  with<sup>4</sup>

$$r_N^2 = \frac{1}{N} \int d^2x \Psi^2(\vec{x}) \vec{x}^2, \quad (13)$$

which is one of the hallmarks of the universal bound states in 2D. For weak interactions, the ratio corresponds to non-interacting bosons in a harmonic oscillator ( $r_{N+1}^2/r_N^2 = 1$ ) while for strong interactions we recover the universal ratio predicted in Ref. [1] ( $r_{N+1}^2/r_N^2 = 0.116$ ). In between these limits, we see that the ratio first increases to values slightly higher than unity and then decreases rapidly. The sudden increase is an artifact of

<sup>3</sup> Here, we assume that there is no symmetry present that can lead to a crossing of energy levels.

<sup>4</sup> Note that  $\Psi(\vec{x})$  depends on  $N$ , see Eq. (3).

our ansatz which is caused by the transition from the trap-dominant to the interaction-dominant states which happens for larger particle numbers for weaker interactions (as can be seen from the figure). It can be explained by the minimization procedure: As soon as the two-body binding energy is large enough such that  $R_{\text{free}} \leq l_{\text{HO}}$ , we have a state dominated by the interactions. Now, we can calculate the mean-square radius for  $R_{\text{free}} = l_{\text{HO}}$

$$r_N^2 = 2\pi l_{\text{HO}}^2 \int d\rho \rho^3 f_{\text{free}}^2(\rho) \approx 1.2l_{\text{HO}}^2, \quad (14)$$

i.e., the maximum value of  $r_{N+1}^2/r_N^2$  we observe. The decrease of the ratio that follows happens when the  $N+1$  system is dominated by the interactions, while the  $N$  system is still in an oscillator state.

Further, Fig. 3 confirms our estimate for the transition point from perturbation theory, Eq. (12). Indeed, according to these data, the transition occurs approximately at  $\ln(B_2/\omega)/N \approx -2.2$  for all particle numbers. A weak dependence on  $N$  is visible only for small systems; for large values of  $N$ , the transition point converges towards the value expected from Eq. (12).

Due to the logarithmic scaling with  $B_2/\omega$ , very large values of the scattering length  $a \propto B_2^{-1/2}$  with a high precision are needed to detect the transition. Here, the harmonic trapping confinement can help to alleviate this issue: One can tune the value  $B_2/\omega$  also by changing the trapping frequency. This additional degree of freedom might facilitate experimental studies of this transition.

### B. Transition indicator: static response

Even with the help of tuning both, the trapping frequency and the scattering length, detecting the transition through the ratio of the mean-square radii (or also the energies) might be very challenging. One must not only maintain high level of control over the experimental parameters (either  $B_2$  or  $\omega$ ), but do so for two experimental runs with different particle numbers. In this subsection, we note that the information about the transition between the two states could actually be extracted in experiments that operate with a single value of  $N$ . We demonstrate this fact by introducing an observable motivated by the standard description of phase transitions. It is also an illustration of a general fact that concepts developed for the description of phases in the thermodynamic limit could be adapted for distinguishing the two states of our system, even though it is finite.

Here, we use the compressibility, which is one of the standard markers of phase transitions [22]. Using linear response theory, one can show that the compressibility of a (uniform) system is strongly related to the so-called static response (or polarizability)  $\chi$  which describes the response of a system's density to a static force field<sup>5</sup> [11].

<sup>5</sup> This is known under the name of the compressibility sum rule.

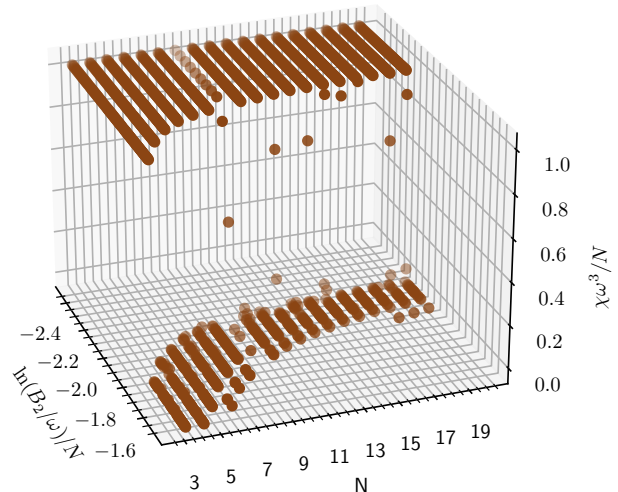


FIG. 4. Static response per particle,  $\chi\omega^3/N$ , see Eq. (15), as a function of the interaction strength  $\ln(B_2/\omega)/N$  and particle numbers  $N$ . All points are calculated with our variational ansatz, Eq. (6). Note that the calculation of the static response close to the transition point requires a high numerical precision for the evaluation of the derivative, see Eq. (15).

For a harmonically trapped system, we can directly calculate  $\chi$  from the change of the mean-square radius upon varying the trapping frequency (in this case  $\chi$  is also called monopole compressibility) [12, 13]:

Let us consider a small change in the trapping frequency  $\epsilon r^2$ . In this case, the static response  $\chi$  is given by  $\delta \langle r^2 \rangle = \epsilon \chi$ , which can be expressed as<sup>6</sup>

$$\chi = -2N \frac{\partial \langle r^2 \rangle}{\partial (\omega^2)}. \quad (15)$$

This quantity allow us to distinguish the two different phases without relying on the ratios of energies or radii, which can certainly make a detection of the transition point significantly easier.

For weak interactions, our system is described by the harmonic oscillator ground state whose mean-square radius naturally follows the trapping frequency. Therefore, we expect the static response to be  $\chi\omega^3 = N$ . In the opposite limit of strong interactions, we can use the result of Ref. [1] and approximate the behavior  $\langle r^2 \rangle \propto \frac{1}{B_2}$ , i.e. there is no influence of the trapping frequency on the

<sup>6</sup> In practice, it might be more convenient to perform calculations using a system of units in which  $\omega = 1$ . To calculate  $\chi$  in this case, one should express the derivative with respect to the trapping frequency in terms of a derivative with respect to  $B_2$ , the interaction strength parameter. This transformation leads to the following definition of  $\chi$ :  $\chi = N \left( B_2 \frac{\partial \langle r^2 \rangle}{\partial B_2} + \langle r^2 \rangle \right)$ .

state and hence  $\chi = 0$ . Therefore, the static response does indeed show a very different behavior for the two states of our system and can be used as an indicator for the transition.

We show a plot of the static response obtained from the minimization procedure in Fig. 4. We see exactly the behavior discussed above: For weak interactions, the static response remains constant at  $\chi\omega^3/N = 1$  up until the transition point. After that, the static response is zero (within our numerical accuracy). Therefore, the observable  $\chi$  allows one to see that a) there is a transition between two different states of the system with very different properties, b) that the interaction strength needed for the transition converges towards  $\ln(B_2/\omega)/N \approx -2.15$  with increasing particle numbers, in agreement with our estimate from perturbation theory, Eq. (12).

### C. Influence of finite range effects

Even though zero-range potentials describe cold-atom systems faithfully [15, 16], it is known that in two-dimensional systems already small effective range corrections can have a large impact on the properties of a few-body system. For an example see, e.g., Ref. [20], which considers a three-boson system in free space. Therefore, one should study the influence of finite range effects on the transition discussed above<sup>7</sup>. To this end, we employ a Gaussian potential of finite width, Eq. (8), and perform *ab initio* calculations with the CI method, see Sec. II B.

We use widths of the Gaussian potential in the order of the harmonic oscillator length,  $\sigma = l_{\text{HO}}/2$  and  $\sigma = l_{\text{HO}}$ . These values cause significant effective range corrections as we will show below. At the same time, the width of the potential acts as a momentum space cut-off, enabling *ab initio* calculations with the CI method within the transition region. Note that for strong attractive interactions, such calculations become computationally very expensive. Therefore, it is challenging to explore the (quasi-)zero-range limit with Gaussian interactions<sup>8</sup>. Nevertheless, by comparing the two widths, we can discuss the finite range effects on the transition.

Let us first estimate the size of the finite range corrections. We show in Fig. 5 the ratio of the effective range and the scattering length as a function of  $B_2/\omega$ <sup>9</sup>. As one can clearly see, the role of the effective range can be very large for these parameters. Indeed, for all considered values of  $B_2/\omega$  the influence of the effective range cannot

be neglected. Furthermore, Eq. (9) only considers finite range corrections up to the effective range. Since the values of the effective range are so large, higher order terms such as the shape parameter might also be important. However, for our study, the calculation of such terms is not important as we are only interested in comparing the size of the finite range effects for different values of  $\sigma$ . For the smaller value of  $\sigma$  one can see that the effective range for the same value of  $B_2/\omega$  is smaller, implying that finite range effects are less important.

In Fig. 5 we present the static response for  $N = 3, 4$  particles for the two different widths of the Gaussian potential as a function of  $\ln(B_2/\omega)/N$ . We can see that the static response does decrease with increasing binding energy. Since we now perform an *ab initio* calculation with a finite-range potential, we do not see a sharp transition for such small particle numbers as in the previous section. Instead, we see a stronger decay of the static response for larger particle numbers. In Ref. [14] a sharper transition between a localized droplet state and a homogeneously distributed state was observed when the particle number was increased for a zero-range potential. The effects of the finite range are visible by comparing the results for the two values of  $\sigma$ . For the larger value, the decrease of the static response is pushed towards larger values of the binding energy. Indeed, comparing with the critical interaction strength  $\ln(B_2/\omega)/N \approx -2.15$ , we can see that significantly stronger attraction is needed for a decrease in the static response. However, further *ab initio* calculations with larger particle numbers and smaller finite ranges are needed to recover the critical transition binding energy described above and to further test how strong the impact of the finite range corrections are.

## IV. SUMMARY AND OUTLOOK

In this work we studied the transition of attractively interacting bosons in a two-dimensional harmonic oscillator from a trap-dominant state (the ground state of a harmonic oscillator) for weak interactions to a universal many-body bound state for strong interactions. With a physically motivated variational ansatz, we showed that this transition happens at  $\ln(B_2/\omega)/N \simeq 2.15$  for large particle numbers. We argued that the transition can be driven by experimentally varying two parameters: The scattering length and the trapping frequency. Further, the classical description of phase transitions motivated us to study the static response – an observable closely related to isothermal compressibility. We showed that it varies significantly between the two states and argued that it can be used as an indicator of the transition. Finally, we discussed the influence of finite range effects in few-body *ab initio* calculations with the configuration interaction method. We found that large finite range effects modify the point of transition.

Further *ab initio* calculations with finite range interactions are needed to better understand their influence

<sup>7</sup> Note that for large finite range effects, the many-body bound state is no longer universal, see Ref. [1]

<sup>8</sup> In practice, weak attractive interactions can pose challenges as well, since we calculate the two-body binding energy numerically. For weak interactions, this energy becomes exponentially small [23], causing loss of accuracy in numerical calculations.

<sup>9</sup> Note that the oscillator units enter via the width of the Gaussian potential which we define with respect to  $l_{\text{HO}}$ .

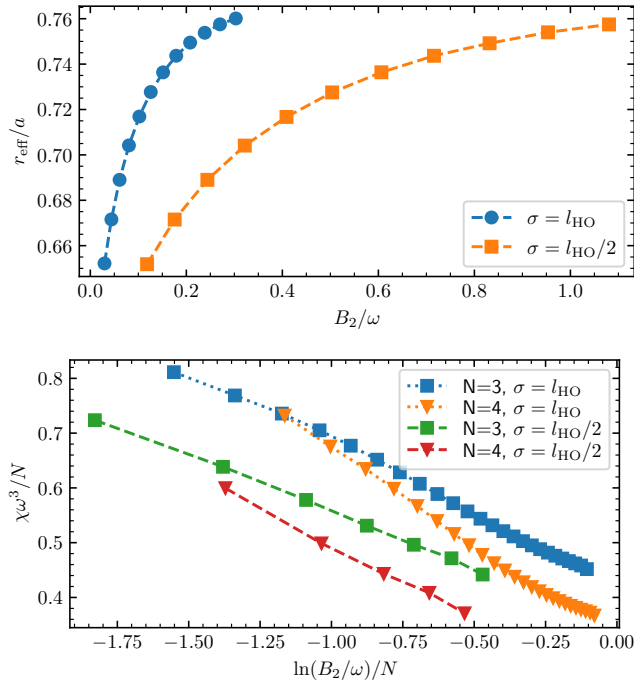


FIG. 5. Upper panel: Ratio of effective range and the scattering length as a function of  $B_2/\omega$  for a Gaussian potential with  $\sigma = l_{\text{HO}}/2$  and  $\sigma = l_{\text{HO}}$ . Lower panel: Static response per particle, Eq. (15), calculated with a CI method as a function of the interaction strength given by  $\ln(B_2/\omega)/N$  (for details on the method see App. B). For the interaction we use a Gaussian potential, Eq. (8). Squares show results for  $\sigma = l_{\text{HO}}$  while triangles are for  $\sigma = l_{\text{HO}}/2$ . The dashed (dotted) lines are added to guide the eye.

on the transition, in particular since Ref. [20] showcases strong influence of finite range effects for the three-body

system in free space. Such calculations might also be important for corresponding experimental studies. Therefore, more sophisticated truncation schemes such as the importance-truncation CI should be employed (see e.g. Refs. [24–26] for applications in the context of ultracold atoms). Furthermore, techniques such as renormalized interactions can be useful to improve the convergence. This might allow one to go to stronger interactions and/or smaller Gaussian potentials [27, 28]. Alternatively, Monte-Carlo calculations with finite range interactions could be used for the study.

Another interesting feature is the increase in sharpness of the transition predicted by Ref. [14]. It would be worthwhile establishing when the transition of our few-body system can be treated as a genuine phase transition. Then one could determine its order and study the dependence on external parameters such as the trapping potential. Furthermore, Ref. [14] and our work focused on the ground state of the system. However, excited states might also provide valuable insight into the (phase) transition like in Ref. [6, 29] where excited states for a finite system were interpreted as precursors of a Higgs mode. We leave such studies to future work.

## ACKNOWLEDGEMENTS

We thank Stephanie Reimann and the Lund cold atom group for giving us access to their configuration interaction code. We thank Michał Suchorowski for useful discussions. H.W.H. was supported in part by Deutsche Forschungsgemeinschaft (DFG, German Research Foundation) - Project-ID 279384907 - SFB 1245 and by the German Federal Ministry of Education and Research (BMBF) (Grants No. 05P21RDFNB and 05P24RDB).

## Appendix A: Details on the variational ansatz

In this Appendix, we provide additional details on the variational ansatz. In particular, we present all relevant equations. For better readability, we use a system of units with  $\hbar = m = \omega = 1$  here. The explicit form of the variational ansatz is

$$\Psi(\vec{r}) = \frac{1}{\sqrt{\alpha_{\text{HO}}^2 + \alpha_{\text{free}}^2 + 2\alpha_{\text{HO}}\alpha_{\text{free}}\frac{\bar{C}}{\sqrt{C}C_2R}}} \left( \alpha_{\text{HO}} \frac{\sqrt{N}}{\sqrt{2\pi}C_2} f_{\text{HO}}(r) + \alpha_{\text{free}} \frac{\sqrt{N}}{\sqrt{2\pi}CR} f_{\text{free}}(r/R) \right) \quad (\text{A1})$$

$$C_2 = \int dr r f_{\text{HO}}^2(r), \quad \bar{C} = \int dr r f_{\text{HO}}(r) f_{\text{free}}(r/R).$$

This ansatz leads to the following expectation value of the Hamiltonian

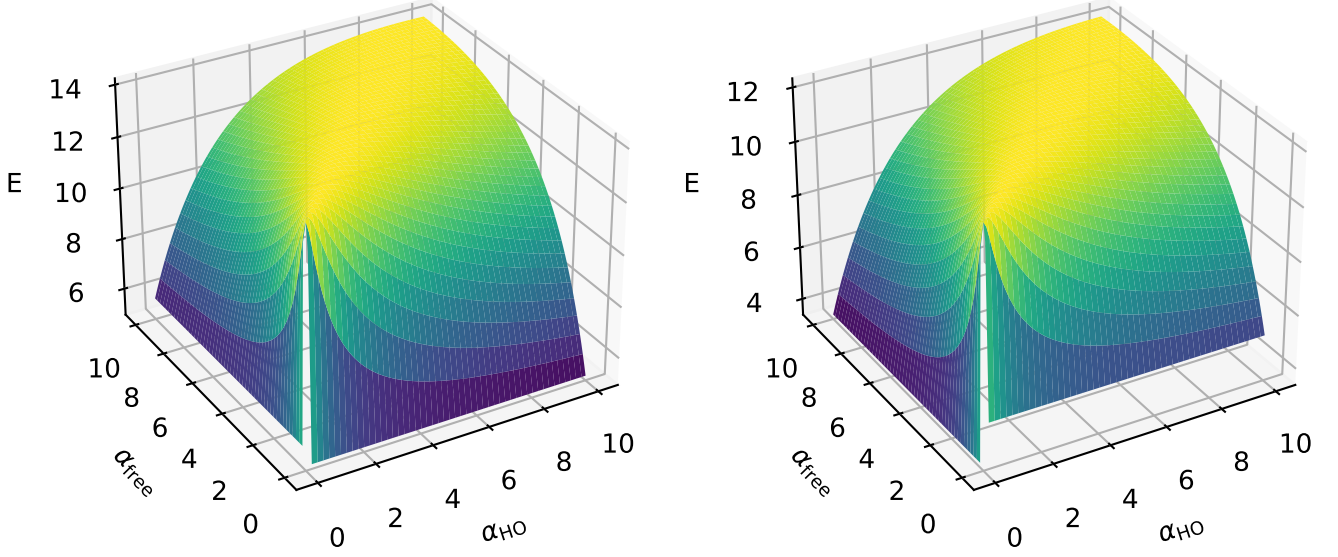


FIG. 6. Energy calculated with our ansatz, Eq. (A2) as a function of the parameters  $\alpha_{\text{HO}}$  and  $\alpha_{\text{free}}$  for  $N = 9$  bosons. The left panel is for  $\ln(B_2)/N = -2.05$ ; the right panel is for  $\ln(B_2)/N = -2$ . Note that both  $\alpha$ -parameters are defined to be positive.

$$\begin{aligned}
E = & \frac{\alpha_{\text{HO}}^2}{\alpha_{\text{HO}}^2 + \alpha_{\text{free}}^2 + 2\alpha_{\text{HO}}\alpha_{\text{free}}\frac{\bar{C}}{\sqrt{CC_2R}}} \left( \frac{N}{2C_2} A_2 - \frac{\alpha_{\text{HO}}^2}{\alpha_{\text{HO}}^2 + \alpha_{\text{free}}^2 + 2\alpha_{\text{HO}}\alpha_{\text{free}}\frac{\bar{C}}{\sqrt{CC_2R}}} \frac{gN^2 B_2}{4\pi C_2} + \frac{1}{2} \frac{ND_2}{C_2} \right) \\
& + \frac{\alpha_{\text{free}}^2}{\alpha_{\text{HO}}^2 + \alpha_{\text{free}}^2 + 2\alpha_{\text{HO}}\alpha_{\text{free}}\frac{\bar{C}}{\sqrt{CC_2R}}} \left( \frac{N}{2C_2 R^2} A - \frac{\alpha_{\text{free}}^2}{\alpha_{\text{HO}}^2 + \alpha_{\text{free}}^2 + 2\alpha_{\text{HO}}\alpha_{\text{free}}\frac{\bar{C}}{\sqrt{CC_2R}}} \frac{gN^2 B}{4\pi C R^2} + \frac{1}{2} \frac{NDR^2}{C} \right) \\
& + 2 \frac{\alpha_{\text{HO}}\alpha_{\text{free}}}{\alpha_{\text{HO}}^2 + \alpha_{\text{free}}^2 + 2\alpha_{\text{HO}}\alpha_{\text{free}}\frac{\bar{C}}{\sqrt{CC_2R}}} \left( \frac{N}{2\sqrt{CC_2}} \tilde{A} + \frac{1}{2} \frac{N}{\sqrt{CC_2}} \tilde{D} \right) \\
& + \frac{\alpha_{\text{HO}}\alpha_{\text{free}}}{\left( \alpha_{\text{HO}}^2 + \alpha_{\text{free}}^2 + 2\alpha_{\text{HO}}\alpha_{\text{free}}\frac{\bar{C}}{\sqrt{CC_2R}} \right)^2} \frac{gN^2}{4\pi} \left( 4 \frac{\alpha_{\text{HO}}^2}{\sqrt{C_2^3 C}} \tilde{B} + 4 \frac{\alpha_{\text{free}}^2}{\sqrt{C_2 C^3}} \bar{B} + 6 \frac{\alpha_{\text{free}}\alpha_{\text{HO}}}{\sqrt{C_2^2 C^2}} \hat{B} \right)
\end{aligned} \tag{A2}$$

with

$$\begin{aligned}
A &= \int dr r [f'_{\text{HO}}(r)]^2, & B_2 &= \int dr r f_{\text{HO}}^4(r), & D_2 &= \int dr r^3 f_{\text{HO}}^2(r) \\
\tilde{A} &= \int dr r f'_{\text{HO}}(r) f'_{\text{free}}(r/R), & \tilde{D} &= \int dr r^3 f_{\text{HO}}(r) f_{\text{free}}(r/R) \\
\tilde{B} &= \int dr r f_{\text{HO}}^3(r) f_{\text{free}}(r/R), & \bar{B} &= \int dr r f_{\text{HO}}(r) f_{\text{free}}^3(r/R), & \hat{B} &= \int dr r f_{\text{HO}}^2(r) f_{\text{free}}^2(r/R).
\end{aligned}$$

To facilitate the calculation of the  $R$ -dependent integrals in each step of the minimization calculation, we assume that  $R = R_{\text{free}}$  if  $R_{\text{free}} < 1$  and in all other cases that  $R = 1$  (see the main text). Next, we minimize the energy, Eq. (A2), with respect to  $\alpha_{\text{HO}}$  and  $\alpha_{\text{free}}$  for each interaction strength. We show a plot of the energy as a function of these parameters in Fig. 6 for two different interaction strengths, for  $R_{\text{free}} > 1$  (left panel) and for  $R_{\text{free}} < 1$  (right panel). We can see that the energy is minimized at the boundaries of the plot, i.e., when one of the parameters is zero. For the left panel with  $R_{\text{free}} > 1$  we can see that it is energetically favorable to have a finite value of  $\alpha_{\text{HO}}$  while in the right one  $\alpha_{\text{free}}$  is preferred. This implies the sharp transition discussed in the main text; there is no particle number or interaction strength for which both  $\alpha$ -values are non-zero after the minimization of the energy.



## Appendix B: Details on the configuration interaction method

For the CI calculations, we write the Hamiltonian in the formalism of second quantization:

$$H = \sum_{i,j} A_{ij} a_i^\dagger a_j + \sum_{i,j,k,l} V_{ijkl} a_i^\dagger a_j^\dagger a_l a_k, \quad (\text{B1})$$

with  $a_i^\dagger$  ( $a_i$ ) bosonic creation (annihilation) operators. We find the one-body matrix  $A_{ij}$  and the two-body matrix  $V_{ijkl}$  by expanding them in one-body basis functions. For these functions, we use the eigenfunctions of the non-interacting system, i.e. the eigenfunctions of the 2D harmonic oscillator (for better readability, we use a system of units such that  $\hbar = m = \omega = 1$ ):

$$\Phi_i(\vec{x}) = \frac{1}{\sqrt{2\pi}} e^{im_i\phi} F_{n_i, m_i}(\rho) = \frac{1}{\sqrt{2\pi}} e^{im_i\phi} (-1)^{n_i} \sqrt{\frac{2\Gamma(n_i + 1)}{\Gamma(|m_i| + n_i + 1)}} e^{-\rho^2/2} \rho^{|m_i|} L_{n_i}^{|m_i|}(\rho^2). \quad (\text{B2})$$

The index  $i$  is the index of the basis state and  $m_i$  is the angular component of this index and  $n_i$  the radial one. We use polar coordinates with  $\rho$  and  $\phi$ .  $L$  is the generalized Laguerre polynomial. Such a state has an eigenenergy of

$$E_{m_i, n_i} = 2n_i + |m_i| + 1. \quad (\text{B3})$$

In the CI-method, we first construct  $N$ -particle basis states, which are then used to write the Hamiltonian matrix for a given set of parameters. This matrix is diagonalized using the Arnoldi/Lanczos method [30].

We must truncate the Hamiltonian matrix in numerical calculations. Therefore, we introduce a one-body basis cutoff such that we include only one-body basis states whose energy is equal or lower to thirteen. To retrieve the two-body energy in free space,  $B_2 = -E_2$ , we solve the Schrödinger equation in relative coordinates (effectively a one-body problem) with up to 500 basis states. Furthermore, as our interaction conserves the total momentum, we only include many-body basis states with a total angular momentum of zero. Attractive interactions localize the bosons in the center of the trap, and many basis states are needed to resolve the ground state. To account for this in our calculations, we use a trapping frequency for the one-body basis, which is different from  $\omega$ :  $\omega_{\text{basis}} = 4\omega$ . This allows us to obtain converged results for stronger interactions. For a detailed explanation of the employed CI-method we refer to Refs. [18, 19].

- 
- [1] H.-W. Hammer and D. T. Son, Universal properties of two-dimensional boson droplets, *Phys. Rev. Lett.* **93**, 250408 (2004).
  - [2] D. Blume, Threshold behavior of bosonic two-dimensional few-body systems, *Phys. Rev. B* **72**, 094510 (2005).
  - [3] D. Lee, Large- $n$  droplets in two dimensions, *Phys. Rev. A* **73**, 063204 (2006).
  - [4] B. Bazak and D. S. Petrov, Energy of  $n$  two-dimensional bosons with zero-range interactions, *New Journal of Physics* **20**, 023045 (2018).
  - [5] Z. Hadzibabic and J. Dalibard, Two-dimensional bose fluids: An atomic physics perspective, *La Rivista del Nuovo Cimento* **34**, 389 (2011).
  - [6] L. Bayha, M. Holten, R. Klemt, K. Subramanian, J. Bjerlin, S. M. Reimann, G. M. Bruun, P. M. Preiss, and S. Jochim, Observing the emergence of a quantum phase transition shell by shell, *Nature* **587**, 583 (2020).
  - [7] M. Holten, L. Bayha, K. Subramanian, C. Heintze, P. M. Preiss, and S. Jochim, Observation of pauli crystals, *Phys. Rev. Lett.* **126**, 020401 (2021).
  - [8] M. Holten, L. Bayha, K. Subramanian, S. Brandstetter, C. Heintze, P. Lunt, P. M. Preiss, and S. Jochim, Observation of cooper pairs in a mesoscopic two-dimensional fermi gas, *Nature* **606**, 287 (2022).
  - [9] S. Brandstetter, P. Lunt, C. Heintze, G. Giacalone, L. H. Heyen, M. Galka, K. Subramanian, M. Holten, P. M. Preiss, S. Floerchinger, and S. Jochim, Emergent hydrodynamic behaviour of few strongly interacting fermions (2023), arXiv:2308.09699 [cond-mat.quant-gas].
  - [10] C. Chin, R. Grimm, P. Julienne, and E. Tiesinga, Feshbach resonances in ultracold gases, *Rev. Mod. Phys.* **82**, 1225 (2010).
  - [11] D. Pines, *The theory of quantum liquids : 1. Normal Fermi liquids*, repr. of the 1966 ed., 3rd print. ed. (Avalon Publishing, Redwood City, Calif., 1994).
  - [12] F. Dalfovo, S. Giorgini, L. P. Pitaevskii, and S. Stringari, Theory of bose-einstein condensation in trapped gases, *Rev. Mod. Phys.* **71**, 463 (1999).
  - [13] L. Pitaevskii and S. Stringari, *Bose-Einstein Condensation and Superfluidity* (Oxford University Press, 2016).
  - [14] A. Tononi, G. E. Astrakharchik, and D. S. Petrov, Gas-to-soliton transition of attractive bosons on a spherical surface, *AVS Quantum Science* **6**, 023201 (2024).
  - [15] E. Braaten and H.-W. Hammer, Universality in few-body systems with large scattering length, *Physics Reports* **428**, 259 (2006).

- [16] I. Bloch, J. Dalibard, and W. Zwerger, Many-body physics with ultracold gases, *Rev. Mod. Phys.* **80**, 885 (2008).
- [17] B. J. Verhaar, J. P. H. W. van den Eijnde, M. A. J. Voermans, and M. M. J. Schaffrath, Scattering length and effective range in two dimensions: application to adsorbed hydrogen atoms, *Journal of Physics A: Mathematical and General* **17**, 595 (1984).
- [18] J. Cremon, *Quantum Few-Body Physics with the Configuration Interaction Approach: Method Development and Application to Physical Systems*, Doctoral thesis (compilation), *Mathematical Physics* (2010).
- [19] J. Bjerlin, *Few- to many-body physics in ultracold gases: An exact diagonalization approach*, Doctoral thesis (compilation), *Mathematical Physics* (2017).
- [20] K. Helfrich and H.-W. Hammer, Resonant three-body physics in two spatial dimensions, *Phys. Rev. A* **83**, 052703 (2011).
- [21] P. Jezszeszki, A. Y. Cherny, and J. Brand, *s*-wave scattering length of a gaussian potential, *Phys. Rev. A* **97**, 042708 (2018).
- [22] F. Schwabl, *Statistical Mechanics*, 2nd ed., *Advanced Texts in Physics* (Springer Berlin Heidelberg, Berlin, Heidelberg, 2006).
- [23] B. Simon, The bound state of weakly coupled schrödinger operators in one and two dimensions, *Annals of Physics* **97**, 279–288 (1976).
- [24] R. Roth, Importance truncation for large-scale configuration interaction approaches, *Phys. Rev. C* **79**, 064324 (2009).
- [25] L. Chergui, J. Bengtsson, J. Bjerlin, P. Stürmer, G. M. Kavoulakis, and S. M. Reimann, Superfluid-droplet crossover in a binary boson mixture on a ring: Exact diagonalization solutions for few-particle systems in one dimension, *Phys. Rev. A* **108**, 023313 (2023).
- [26] J. Bengtsson, G. Eriksson, J. Josefi, J. C. Cremon, and S. M. Reimann, Interplay between shell structure and trap deformation in dipolar Fermi gases, *Phys. Rev. A* **102**, 053302 (2020).
- [27] J. Christensson, C. Forssén, S. Åberg, and S. M. Reimann, Effective-interaction approach to the many-boson problem, *Phys. Rev. A* **79**, 012707 (2009).
- [28] F. Brauneis, H.-W. Hammer, S. M. Reimann, and A. G. Volosniev, Comparison of renormalized interactions using one-dimensional few-body systems as a testbed (2024), arXiv:2408.10052 [cond-mat.quant-gas].
- [29] J. Bjerlin, S. M. Reimann, and G. M. Bruun, Few-body precursor of the higgs mode in a fermi gas, *Phys. Rev. Lett.* **116**, 155302 (2016).
- [30] G. Golub and C. Van Loan, *Matrix computations* (1996).